

PPPL-5381

## Elimination of Inter-discharge Helium Glow Discharge Cleaning with Lithium Evaporation in NSTX

R. Maingi, R. Kaita, and the NSTX team

April 2017



Prepared for the U.S. Department of Energy under Contract DE-AC02-09CH11466.

# Princeton Plasma Physics Laboratory

## Report Disclaimers

---

### Full Legal Disclaimer

This report was prepared as an account of work sponsored by an agency of the United States Government. Neither the United States Government nor any agency thereof, nor any of their employees, nor any of their contractors, subcontractors or their employees, makes any warranty, express or implied, or assumes any legal liability or responsibility for the accuracy, completeness, or any third party's use or the results of such use of any information, apparatus, product, or process disclosed, or represents that its use would not infringe privately owned rights. Reference herein to any specific commercial product, process, or service by trade name, trademark, manufacturer, or otherwise, does not necessarily constitute or imply its endorsement, recommendation, or favoring by the United States Government or any agency thereof or its contractors or subcontractors. The views and opinions of authors expressed herein do not necessarily state or reflect those of the United States Government or any agency thereof.

### Trademark Disclaimer

Reference herein to any specific commercial product, process, or service by trade name, trademark, manufacturer, or otherwise, does not necessarily constitute or imply its endorsement, recommendation, or favoring by the United States Government or any agency thereof or its contractors or subcontractors.

---

## PPPL Report Availability

### Princeton Plasma Physics Laboratory:

<http://www.pppl.gov/techreports.cfm>

### Office of Scientific and Technical Information (OSTI):

<http://www.osti.gov/scitech/>

---

### Related Links:

[U.S. Department of Energy](#)

[U.S. Department of Energy Office of Science](#)

[U.S. Department of Energy Office of Fusion Energy Sciences](#)

## Elimination of Inter-discharge Helium Glow Discharge Cleaning with Lithium Evaporation in NSTX

**R. Maingi<sup>a</sup>**, R. Kaita<sup>a</sup>, F. Scotti<sup>b</sup>, V.A. Soukhanovskii<sup>b</sup>, and the NSTX team

<sup>a</sup> Princeton Plasma Physics Laboratory, Receiving 3, Route 1 North, Princeton, NJ 08543 USA

<sup>b</sup> Lawrence Livermore National Laboratory, 7000 East Ave, P.O. Box 808, Livermore CA 94551, USA

Operation in the National Spherical Torus Experiment (NSTX) typically used either periodic boronization and inter-shot helium glow discharge cleaning (HeGDC), or inter-shot lithium evaporation without boronization, and initially with inter-shot HeGDC. To assess the viability of operation without HeGDC, dedicated experiments were conducted in which Li evaporation was used while systematically shrinking the HeGDC between shots from the standard 10 minutes to zero (10 → 6.5 → 4 → 0). Good shot reproducibility without HeGDC was achieved with lithium evaporations of 100 mg or higher; evaporations of 200-300 mg typically resulted in very low ELM frequency or ELM-free operation, reduced wall fueling, and improved energy confinement. The use of HeGDC before lithium evaporation modestly reduced  $D_{\alpha}$  in the outer scrape-off layer, but not at the strike point. Pedestal electron and ion temperature also improved modestly, suggesting that HeGDC prior to lithium evaporation is a useful tool for experiments that seek to maximize plasma performance.

PACS: 52.40.Hf, 52.25.-b, 52.30.-q, 52.55.-s

PSI21 Keywords: NSTX, Lithium, Recycling, Pedestal, Energy Confinement

Corresponding Author Address: PPPL, Receiving 3, Route 1 North, Princeton NJ 08543

Corresponding Author Email: [rmaingi@pppl.gov](mailto:rmaingi@pppl.gov)

Presenting Author and Email: Rajesh Maingi, [rmaingi@pppl.gov](mailto:rmaingi@pppl.gov)

## **I. Introduction**

Fusion devices use a variety of techniques<sup>1</sup> to manage the intense plasma-wall interactions<sup>2</sup> that can reduce plasma performance and/or can damage the wall materials. Two such techniques are the use of wall coatings<sup>3</sup>, applied infrequently or sometimes between discharges, and the use of discharge conditioning between plasma discharges, e.g. helium glow discharge cleaning (HeGDC)<sup>4</sup>. On the National Spherical Torus Experiment (NSTX), helium glow discharge cleaning was routinely used in conjunction with periodic boronizations to reduce oxygen content<sup>5, 6</sup> and provide routine access to H-mode<sup>7</sup>. These early studies of boronized plasmas with inter-discharge HeGDC were followed by studies of lithium injection, first via pellets<sup>8</sup>, and then via evaporation<sup>9</sup>. The evaporative coatings showed an increase in energy confinement<sup>10, 11</sup>, and elimination of Type I ELMs<sup>12</sup>, related to reduced wall fueling and an inward shift of the pedestal density and pressure profiles<sup>13, 14</sup>. While the first of these experiments used HeGDC prior to lithium evaporation, the wall fueling reduction afforded by lithium evaporation<sup>15</sup> raised the prospect of eliminating HeGDC altogether, to simplify operational procedures and reduce the time between discharges. To test this, a sequence of discharges was conducted with the HeGDC time before lithium evaporation reduced sequentially from 10 minutes down to zero, at approximately constant lithium dose, external heating, and fueling. The remainder of this paper describes this systematic HeGDC scan.

## **II. Layout of wall conditioning tools and previous treatments for wall conditioning**

The NSTX plasma-facing components (PFCs) were made of graphite, either ATJ or carbon-fiber composite, and of varying thicknesses from 1.3 to 5.1 cm<sup>16</sup>. Two wall-

mounted anodes were typically used as the HeGDC electrodes for NSTX, separated toroidally by roughly  $120^\circ$  (Figure 1a)<sup>5</sup>. The pair of electrodes typically drew  $\sim 3$  A of current at an applied voltage of 400-500 V, with a He fill pressure  $\sim 3$ -4 mTorr. Typical HeGDC duration was  $\sim 10$  minutes, followed by a few minutes for pump out, and then a 15 minute inter-discharge cycle time. Longer HeGDC durations were tested up to 15 minutes, with a 20-minute inter-discharge cycle time, for experiments that desired the lowest recycling conditions with boronized wall conditions. It should be noted that boronization with tri-methyl boron, which was performed approximately once per month in NSTX, used the same HeGDC system, with a mixture of He and tri-methyl boron injected at a port near the pumping duct<sup>5</sup>. Reproducible ELMy H-mode discharges were obtained in NSTX, including ones with Type I ELMs<sup>17</sup>, using these wall conditioning techniques of periodic boronizations and inter-discharge HeGDC.

An important research element in NSTX was to evaluate the effect of lithium coatings on the carbon PFCs. Initial experiments were done with a single lithium evaporator, which were then extended to two evaporators separated toroidally by about roughly  $150^\circ$  (Figure 1b)<sup>9</sup>. These evaporators deposited lithium in a Gaussian distribution with a  $1/e$  fall-off  $11.5^\circ$  away from the centerline. The deposition rate could be varied between 10 and 70 mg/minute/evaporator, by changing the evaporator operating temperature. A typical discharge sequence used 6.5-10 minutes of HeGDC, followed by 7-8 minutes of lithium evaporation, leading to a  $\sim 20$  minute inter-discharge cycle time. It was found that the Type I ELMs were methodically eliminated<sup>12</sup> and confinement was progressively improved<sup>18</sup> with increasing lithium dose. While these first experiments were conducted

with the combination of HeGDC followed by lithium evaporation, a dedicated experiment in which the HeGDC duration was systematically reduced from 10 minutes to zero at constant lithium evaporation was conducted, as described below.

### **III. Effects of lithium evaporation on wall fueling and local recycling**

The HeGDC duration variation experiment was conducted in highly shaped plasmas: average triangularity  $\delta \sim 0.6-0.7$ , elongation  $\kappa \sim 2.2$ , high squareness, in a near double-null configuration (Figure 2). This configuration was partly chosen because the centroid of the lithium evaporation was close to the outer strike point, which was shown in subsequent experiments to be more effective at reducing wall fueling than configurations where the outer strike point was far from the centroid of lithium deposition<sup>19</sup>. Other discharge parameters were plasma current  $I_p = 0.9$  MA, toroidal field  $B_t = -0.45$  T, ion grad-B drift toward the lower X-point, neutral beam power ( $P_{NBI}$ ) between 4 and 6 MW (although all direct comparisons are made during the 4 MW phases of discharges), and constant external gas fueling.

A comparison of discharge evolution from several relevant discharges with identical external gas fueling is shown in Figure 3. A reference ELMy H-mode, with no lithium evaporation, and taken before any lithium had been deposited in the campaign (129014 – black solid) is compared with a similar discharge (129096 – red dashed) with no direct lithium evaporation (but with 19g of intervening lithium evaporation), and a discharge with  $\sim 500$ mg of lithium evaporation and with 6.5 minutes of HeGDC prior to lithium evaporation (129101 – blue dash dot). Each of these discharges had phases of 4 MW and

6 MW of neutral beam injection (panel (b) -  $P_{\text{NBI}}$ ). The line-average density from Thomson scattering (panel (c)) ramped in all 3 discharges but had the slowest temporal evolution in the one with Li evaporation with preceding HeGDC.  $\beta_{\text{N}}$ , the normalized pressure, is defined as  $\beta_{\text{N}} = \beta_{\text{t}} B_{\text{t}} a_{\text{m}} / I_{\text{p}}$ , where  $\beta_{\text{t}}$  is the average plasma pressure normalized to the on-axis vacuum toroidal field:  $\beta_{\text{t}} = 4\mu_0 W_{\text{MHD}} / (3V_{\text{p}} B_{\text{t}}^2)$ . Here  $B_{\text{t}}$  is the toroidal field,  $a_{\text{m}}$  the minor radius,  $W_{\text{MHD}}$  the stored energy from equilibrium reconstructions,  $V_{\text{p}}$  the plasma volume, and  $\mu_0$  the permittivity of free space. Panel (d) shows that  $\beta_{\text{N}}$  was highest for the discharge with Li and preceding HeGDC, when comparing the 4 MW  $P_{\text{NBI}}$  phases. This is also reflected in the energy confinement time,  $\tau_{\text{E}}$ , normalized to the H97L L-mode scaling<sup>20</sup> (panel (e)). Panel (f) shows that the lower divertor  $D_{\alpha}$  emission is reduced substantially by the presence of lithium in NSTX (i.e. red dash curve lower than black solid curve), and further reduced with application of lithium and HeGDC prior to the discharge. ELM elimination, however, requires the lithium evaporation just before the discharge.

#### **IV. Scan of HeGDC duration preceding Li evaporation**

A systematic scan of the HeGDC time prior to lithium evaporation was conducted, by going from 10 min to 6.5 min to 4 min and then eliminating HeGDC completely. The starting point was an ELM-free H-mode with  $\sim 500$  mg lithium pre-discharge evaporation. A comparison of several of the discharges from the HeGDC duration scan is shown in [Figure 4](#). As can be seen, the plasma evolution was very similar in these discharges, although the reduction of the HeGDC duration at fixed external fueling resulted in a modest decrease of the observed pulse lengths (panel (a)). The discharge

with no HeGDC (#129106 green curves) did have slightly higher radiated power ( $P_{\text{rad}}$ ) and divertor  $D_{\alpha}$  emission (panels (f) and (g)).

The edge electron density, temperature, and ion temperature ( $n_e$ ,  $T_e$ ,  $T_i$ ) profiles at the same line-averaged density are compared for three of the discharges during the HeGDC duration scan in Figure 5. Panel 5(a) confirms that the density profile shape and magnitude was nearly identical for the three chosen time slices. A reduction in the edge  $T_e$  and  $T_i$  of up to 15-30% can be observed in panels (b) and (c), with the biggest reduction observed for the discharge with no HeGDC (#129106 blue diamonds).

As can be seen in panel 4(g), the divertor  $D_{\alpha}$  emission is slightly higher when HeGDC was completely omitted prior to lithium evaporation. The divertor  $D_{\alpha}$  emission radial profile is compared in Figure 6 for the discharges from Figure 4 at a representative time,  $t=0.55$  sec. It can be seen that the peak emission near the outer strike point, i.e. at radius  $\sim 0.35$ m is comparable for the discharges, but that the emission from radius  $> 0.45$  m is markedly higher for the discharge without HeGDC (#129106 – green). We note that the profiles at other times showed these same trends.

To quantify the impact of the radial variations on the total flux, the photon flux was converted to equivalent local ion flux by  $\Gamma = \gamma \int_{R1}^{R2} D_{\alpha}(r) 2\pi R(r) dr$ , where  $\gamma$  is the number of ionizations per photon (assumed to be 20 for an ionizing plasma), for several



discharges from the previous figures. We note that the approximation of 20 ionizations per  $D_\alpha$  photon is necessary because divertor  $n_e$  and  $T_e$  are unavailable for this dataset; the range is 10-30 ionizations per  $D_\alpha$  photon for typical divertor conditions, and thus this approximation is semi-quantitative at best. [Figure 7](#) compares the time evolution of the fluxes for the far SOL profiles (i.e.  $R1 = 0.45\text{m}$ ,  $R2=0.55\text{m}$ , panel (a)) and the near SOL fluxes (i.e.  $R1 = 0.35\text{m}$ ,  $R2=0.45\text{m}$ , panel (b)). As can be seen in [Figure 7a](#), the far SOL particle flux is higher for the discharge without HeGDC (#129106 green) than the ones with 6.5 min HeGDC (129102 blue) and 10 min HeGDC (129100 black). For context, the flux from the discharge with no lithium evaporation and 10 min HeGDC (#129096 orange) is also plotted. [Figure 7b](#) shows that the near SOL particle flux for the three discharges with lithium evaporation are comparable, and all are much lower than for the discharge with no lithium evaporation. One speculation for the similarity in the near SOL flux is that the intense plasma-bombardment near the outer strike point tends to saturate and regulate the surface rapidly, i.e. largely independent of the preceding HeGDC. One possible mechanism for this is that the high PFC temperature near the strike point may hasten the diffusion rate from the bulk back to the surface. However the lower flux in the far SOL for discharges with HeGDC means that the equilibrium surface particle flux can be affected in low fluence zones, i.e. that the HeGDC can reduce  $D_\alpha$  in those regions. It is interesting to note that the flux reduction does not depend on the duration of HeGDC, i.e. deployment of small durations is sufficient for flux control.

There is a natural tendency for the  $D_\alpha$  emission to be equated to recycling, i.e. high  $D_\alpha =$

high recycling. Defining the “local recycling coefficient” as the ratio of  $D_\alpha$  emission (“outflux from the target”) to local ion saturation current from an embedded Langmuir probe (“influx to the target), we find that the “local recycling coefficient” does not change with the HeGDC duration. However if “recycling” is viewed as the ratio of  $D_\alpha$  emission to external fueling, then indeed the discharge with no HeGDC exhibits higher “recycling” than the ones with preceding HeGDC. Thus these results cannot be generically interpreted as “HeGDC reduced recycling”, because the quantification of “recycling” is both difficult and variable depending on the definition.

## **V. Summary and Conclusions**

We have conducted a systematic scan of the HeGDC time, applied before lithium evaporation, in NSTX. At constant external fueling and lithium evaporation, the discharge duration shrank modestly with decreasing HeGDC duration. Moreover the edge  $T_e$  and  $T_i$  decreased moderately with decreasing HeGDC duration at constant density and heating power. On the other hand, the divertor  $D_\alpha$  emission in the far SOL increased when HeGDC was eliminated, but was otherwise unaffected by HeGDC duration. Moreover the near-SOL divertor  $D_\alpha$  emission was unaffected by the duration of HeGDC. Finally with the  $\sim 500\text{mg}$  of lithium dose deployed, all discharges were ELM-free, also independent of the HeGDC duration.

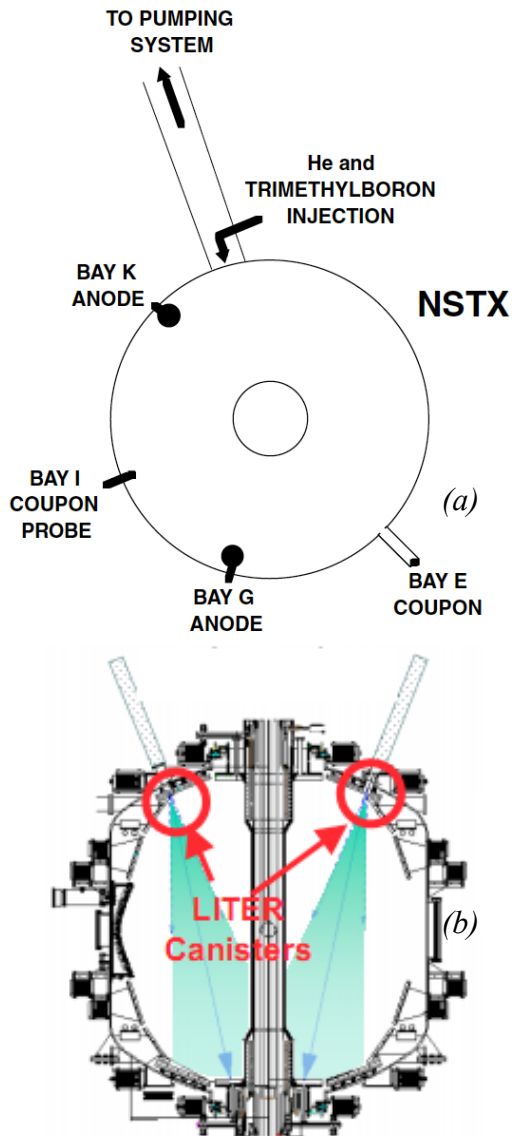
These results have practical implications for NSTX-U<sup>21</sup>. A cycle of 3-5 minutes HeGDC, followed by  $\sim 10$  minutes of lithium evaporation is advocated, as that fits efficiently

within the typical inter-discharge cycle time of 15-20 minutes. On the other hand, experiments that desire the highest performance discharges should deploy longer HeGDC times, albeit at the cost of increasing the inter-discharge cycle time.

### **Acknowledgements**

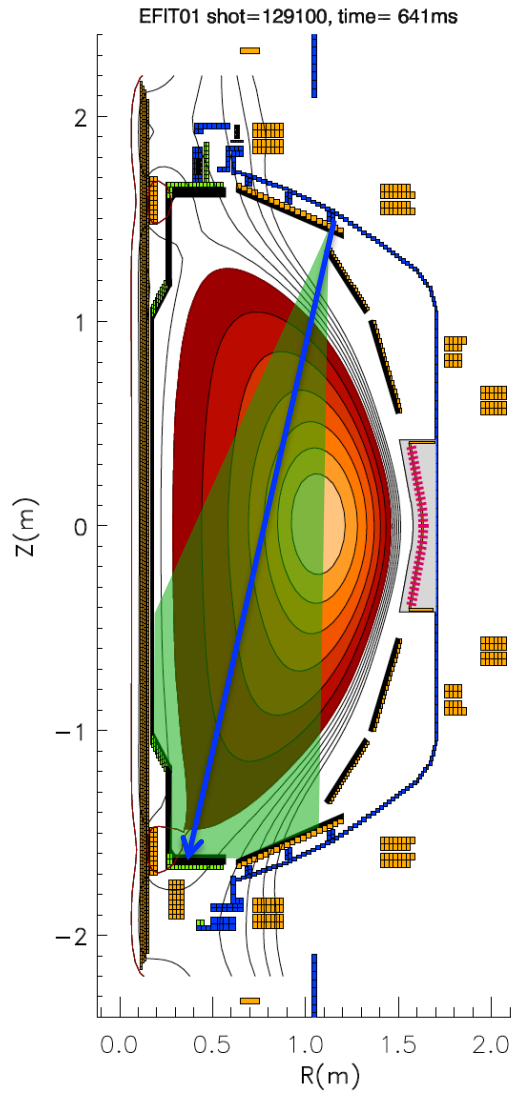
This research was sponsored in part by U.S. Dept. of Energy under contracts DE-AC02-09CH11466, DE-AC05-00OR22725, and DE-AC52-07NA27344. We gratefully acknowledge discussions with C.H. Skinner, and the contributions of the NSTX operations staff.

Figure 1:



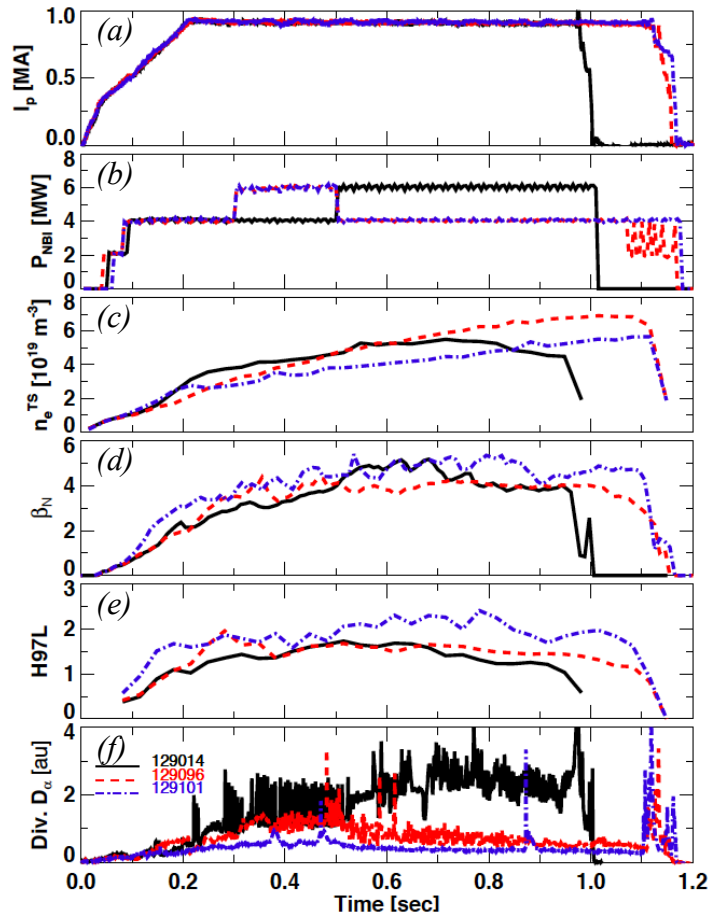
*Fig. 1: (a) plan view of NSTX showing the location of two HeGDC probes used as anodes; (b) poloidal cross-section of NSTX showing two (toroidally separated) lithium evaporators, and the Gaussian width spread of the evaporation cone.*

Figure 2:



*Fig. 2: boundary equilibrium shape with centroid of lithium evaporator deposition for representative discharge from experiment.*

Figure 3:



*Fig. 3: evolution of discharge quantities for three discharges: (a) plasma current  $I_p$ , (b) neutral beam heating power  $P_{NBI}$ , (c) line-averaged density from Thomson Scattering  $n_e^{TS}$ , (d) normalized plasma pressure  $\beta_N$ , (e) energy confinement relative to ITER H97 L-mode scaling, and (f) lower divertor  $D_\alpha$ . See the text for description of discharges.*

Figure 4:

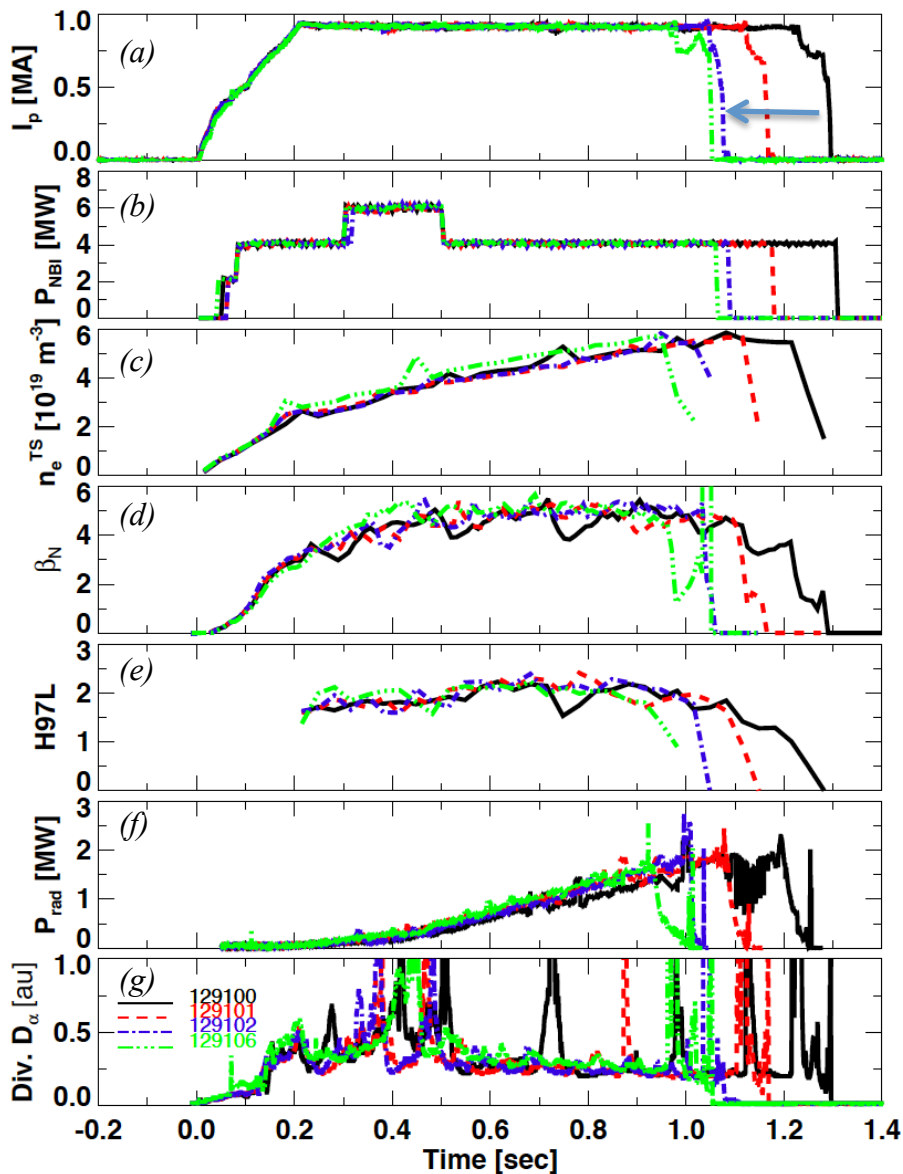


Fig. 4: evolution of discharge quantities for discharges during HeGDC duration scan: (a) plasma current  $I_p$ , (b) neutral beam heating power  $P_{NBI}$ , (c) line-averaged density from Thomson Scattering  $n_e^{TS}$ , (d) normalized plasma pressure  $\beta_N$ , (e) energy confinement relative to ITER H97 L-mode scaling, (f) core radiated power  $P_{rad}$ , and (g) lower divertor  $D_\alpha$ . The duration of HeGDC preceding Li evaporation decreased in the direction of the arrow in panel (a). The color coding is: 10 min HeGDC (black), 6.5 min HeGDC (red), 4 min HeGDC (blue), and no HeGDC (green).

Figure 5:

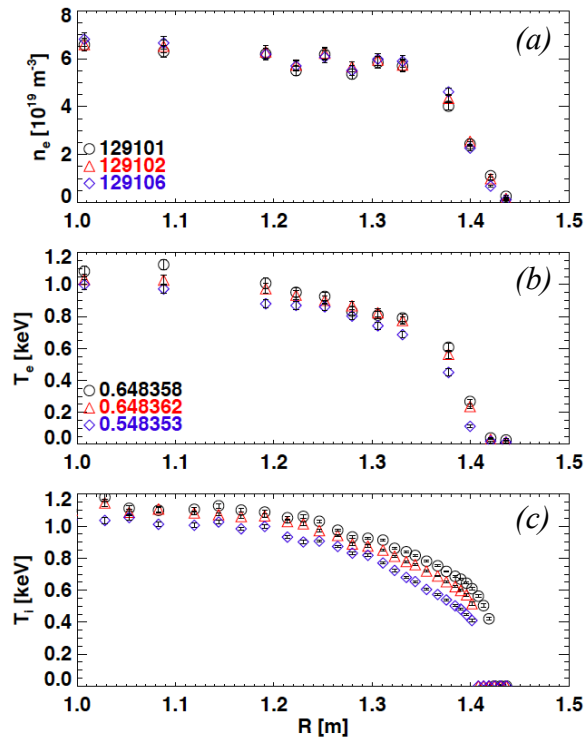
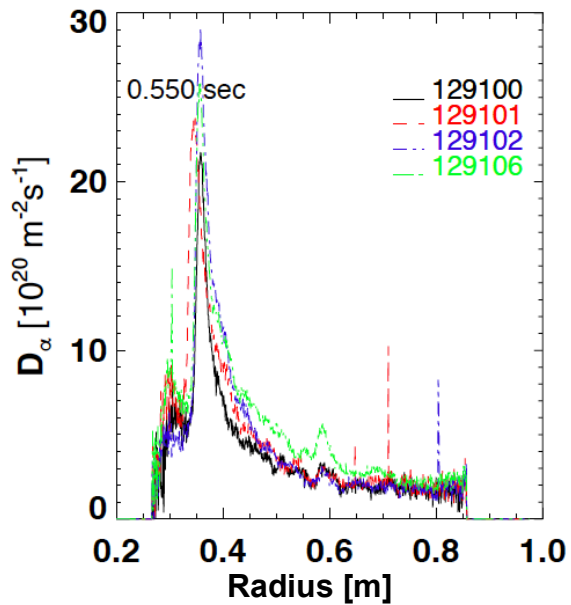


Fig. 5: comparison of  $n_e$ ,  $T_e$ , and  $T_i$  profiles for discharges with 6.5 min HeGDC (black circles), 4 min HeGDC (red triangles), and no HeGDC (blue diamonds). All discharges were followed by comparable amounts of lithium evaporation. The legends in panels (a) and (b) list shot numbers and times used for Thomson profiles.



Figure 6:



*Fig. 6: radial profile of  $D_\alpha$  emission from discharge with 10 min HeGDC (black), 6.5 min HeGDC (red), 4 min HeGDC (blue) and no HeGDC (green). All discharges were followed by comparable amounts of lithium evaporation.*

Figure 7:

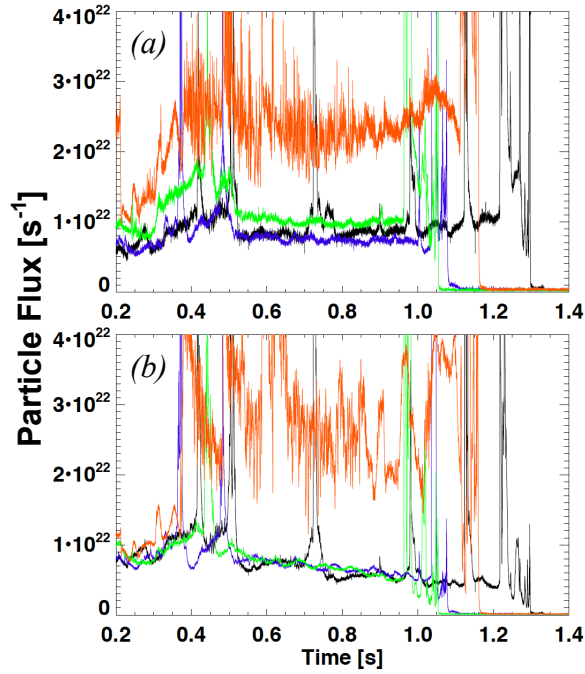


Fig. 7: Equivalent particle flux by integrating  $D_\alpha$  emission in (a) far SOL, and (b) near SOL, from discharges with 10 min HeGDC (black), 6.5 min HeGDC (blue), and no HeGDC (green). Also shown is a discharge with 10 min HeGDC but no Li dose (orange). See the text for additional information.

## References

1. Winter J., *Plasma Phys Control Fusion* **38** (1996) 1503.
2. Federici G., C.H. Skinner, J.N. Brooks, *et al.*, *Nucl Fusion* **41** (2001) 1967.
3. Winter J., *Plasma Phys Control Fusion* **36** (1994) B263.
4. Jackson G.L., T.S. Taylor, and Taylor P. L., *Nucl Fusion* **30** (1990) 2305.
5. Skinner C. H., H.W. Kugel, R. Maingi, *et al.*, *Nucl Fusion* **42** (2002) 329.
6. Kugel H. W., V. Soukhanovskii, M. Bell, *et al.*, *J Nucl Mater* **313** (2003) 187.
7. Maingi R., Bell M., Bell R., *et al.*, *Phys Rev Lett* **88** (2002)
8. Kugel H. W., M.G. Bell, R. Bell, *et al.*, *J Nucl Mater* **363-365** (2007) 791.
9. Kugel H. W., D. Mansfield, R. Maingi, *et al.*, *J Nucl Mater* **390-391** (2009) 1000.
10. Kugel H. W., M. G. Bell, Ahn J.-W., *et al.*, *Phys Plasmas* **15** (2008) 056118.
11. Bell M. G., Kugel H. W., Kaita R., *et al.*, *Plasma Phys Control Fusion* **51** (2009) 124054.
12. Mansfield D. K., Kugel H. W., Maingi R., *et al.*, *J Nucl Mater* **390-391** (2009) 764.
13. Maingi R., T.H. Osborne, LeBlanc B. P., *et al.*, *Phys Rev Lett* **103** (2009) 075001.
14. Canik J. M., Maingi R., Kubota S., *et al.*, *Phys Plasmas* **18** (2011) 056118.
15. Canik J. M., Maingi R., Soukhanovskii V. A., Bell R. E., Kugel H. W., LeBlanc B. P., and Osborne T. H., *J Nucl Mater* **415** (2011) S409.
16. Kugel H. W., R. Maingi, W. Wampler, *et al.*, *J Nucl Mater* **290-293** (2001) 1185.
17. Maingi R., Bush C. E., Fredrickson E. D., *et al.*, *Nucl Fusion* **45** (2005) 1066.
18. Maingi R., Kaye S. M., Skinner C. H., *et al.*, *Phys Rev Lett* **107** (2011) 145004.
19. Maingi R., Osborne T. H., Bell M. G., *et al.*, *J Nucl Mater* **463** (2015) 1134.
20. Kaye S. M., and group t. I. c. d. w., *Nucl Fusion* **37** (1997) 1303.
21. Menard J. E., Gerhardt S., Bell M., *et al.*, *Nucl Fusion* **52** (2012) 083015.

# Princeton Plasma Physics Laboratory Office of Reports and Publications

Managed by  
Princeton University

under contract with the  
U.S. Department of Energy  
(DE-AC02-09CH11466)

---

P.O. Box 451, Princeton, NJ 08543  
Phone: 609-243-2245  
Fax: 609-243-2751

E-mail: [publications@pppl.gov](mailto:publications@pppl.gov)

Website: <http://www.pppl.gov>